Analytica Chimica Acta 1250 (2023) 340952

Contents lists available at ScienceDirect

Analytica Chimica Acta

journal homepage: www.elsevier.com/locate/aca

Simple and rapid formic acid sample treatment for the isolation of HgSe nanoparticles from animal tissues

K. El Hanafi [a,1], B. Gomez-Gomez [b,1], Z. Pedrero [a,*], P. Bustamante [c,d], Y. Cherel [e], D. Amouroux [a], Y. Madrid [b]

[a] Université de Pau et des Pays de l'Adour, E2S UPPA, CNRS, IPREM, Institut des Sciences Analytiques et de Physico-chimie pour l'Environnement et les Matériaux, Pau, France
[b] Departamento de Química Analítica, Facultad de Ciencias Químicas, Universidad Complutense de Madrid, Madrid, 28040, Spain
[c] Littoral Environnement et Sociétés (LIENSs), UMR 7266 CNRS- La Rochelle Université, 2 Rue Olympe de Gouges, 17000, La Rochelle, France
[d] Institut Universitaire de France (IUF), 1 Rue Descartes, 75005, Paris, France
[e] Centre d'Etudes Biologiques de Chizé, UMR 7372 CNRS-La Rochelle Université, 79360, Villiers-en-Bois, France

HIGHLIGHTS

- A novel cost effective and green procedure to extract HgSe nanoparticles from animal tissues with organic acid.
- An alternative to conventional and classical enzymatic procedure with ultrasonic assistance reducing the extraction time from 12 h to 2 min.
- Successfully application of both method (enzymatic and organic acid) to different tissues of seabirds.
- AsNPs and CdNPs were isolated with organic acid method and identified associated with HgSeNPs.
- Perspectives for the application of the novel acid extraction procedure to other metallic nanoparticles from biota.

GRAPHICAL ABSTRACT

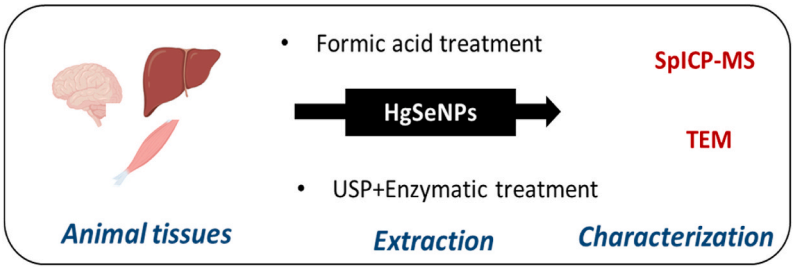

ARTICLE INFO

Prof. W.W. Buchberger

Keywords:
Mercury
Selenium
Tiemannite
spICP-MS
Sample treatment
Seabirds

ABSTRACT

The present work explores for the first time the potential of formic acid on the extraction of tiemannite (HgSe) nanoparticles from seabird tissues, in particular giant petrels. Mercury (Hg) is considered one of the top ten chemicals of major public health concern. However, the fate and metabolic pathways of Hg in living organisms remain unknown. Methylmercury (MeHg), largely produced by microbial activity in the aquatic ecosystems is biomagnified in the trophic web. HgSe is considered the end-product of MeHg demethylation in biota and an increasing number of studies focuses on the characterization of this solid compound to understand its biomineralization. In this study, a conventional enzymatic treatment is compared with a simpler and environmentally friendly extraction by using formic acid (5 mL of = 50 % formic acid) as exclusive reagent. The analyses by spICP-MS of the resulting extracts from a variety of seabird biological tissues (liver, kidneys, brain, muscle) reveal comparable results by both extraction approaches in terms of nanoparticles stability and extraction efficiency. Therefore, the results included in this work demonstrate the good performance of employing organic acid

* Corresponding author.
E-mail address: zoyne.pedrerozayas@univ-pau.fr (Z. Pedrero).
[1] K. El Hanafi, B. Gomez-Gomez, contributed equally.

https://doi.org/10.1016/j.aca.2023.340952
Received 2 December 2022; Received in revised form 3 February 2023; Accepted 6 February 2023
Available online 8 February 2023

as simple, cost effective and green procedure to extract HgSe nanoparticles from animal tissues. Moreover, an alternative consisting of a classical enzymatic procedure but with ultrasonic assistance reducing the extraction time from 12 h to 2 min is also described for the first time. The sample processing methodologies developed, combined with spICP-MS, have emerged as powerful tools for the rapid screening and quantification of HgSe nanoparticles in animal tissues. Finally, this combination allowed us to identify the possible occurrence of Cd particles and As particles associated with HgSe NPs in seabirds.

1. Introduction

In recent years, an exponential number of research focused on the biosynthesis of nanomaterials [1]. Nanoparticles (NPs) can be biosynthesized by different living organisms, from microorganisms to metazoan [1,2]. The study of NPs is a growing field of interest that includes their characterization, bioaccumulation, fate, and interaction with living organisms [3,4]. In animal species, NPs can be biodistributed, reaching key tissues as liver, kidneys, spleen, heart and brain [5–8] without being altered and/or metabolized [9]. The beneficial therapeutic effects and the potential toxicity depend strongly on the properties of the NPs [10], such as their composition, size and shape, which underlines their crucial characterization in biota [11].

Different analytical approaches have been deployed for the characterization of NPs, usually based on the combination of different and complementary techniques [12]. The most widely used are those based on microscopy, such as Transmission Electron Microscopy (TEM), which provides information about size, shape and aggregation/agglomeration state of the NPs. However, the lack of spatial resolution in TEM analysis hampers the complete characterization of NPs in terms of particle concentration [13]. In this sense, Single Particle Inductively Coupled Plasma Mass Spectrometry (spICP-MS) is a promising technique for the characterization, detection, and quantification of NPs [14,15]. Since it allows the determination of their chemical composition, size distribution and particle concentration, which is crucial in toxicological and environmental studies [16]. spICP-MS have been successfully applied in different scenarios like tracking gold (Au) nanomaterials trophic transfer [17], titanium NPs fate in watersheds [18] and silver NPs in environmental samples [19]. Most studies focused on NPs analyses in aqueous matrices [20], probably due to the challenge associated to sample preparation required in biological matrices prior to spICP-MS analyses [21].

NPs sample treatment for isolation prior characterization is a crucial step that must guarantee their preservation and integrity [22]. This stage requires optimization according to the characteristics of the tissue and the type of NPs to be studied. In the case of isolation of NPs from samples of biological origin, usually alkaline (tetramethylammonium hydroxide-TMAH) and enzymatic procedures have been employed [23,24]. However, it is largely documented that enzymatic treatments are sensitive to extraction conditions that influence the enzymatic activity like pH, temperature and reagent compatibility [24,25]. The ratio between sample and enzymes is also a key factor to optimize and such enzymatic treatments are usually quite time consuming, including overnight incubations [12,24]. Proteases are the most common enzymes for the extraction of metallic nanoparticles from animal samples, generally combined with sodium dodecyl sulfate (SDS) as surfactant [24].

Acid treatments have been less exploited so far for NPs isolation, as it could affect the nanoparticle surface [26]. For example, silver and zinc NPs were transformed in terms of size and state (soluble and/or ionic form) in acidic media [26,27] meanwhile the removal of thiol coating of CdSe NPs in $\phi = 0.5\%$ HCl leads to precipitation and aggregation of the NPs [28]. Formic acid is considered an efficient alternative to conventional sample treatments for solubilizing solid biological and other environmental matrices [29]. This organic acid has been successfully used for the extraction of Hg [30] and other trace elements [29] from animal samples [31] and marine sediments [31]. The efficiency of formic acid has been also exploited on the extraction and stabilization of speciation studies of As-peptides in plants [32] and the solubilisation of the membrane proteins [33]. Despite the excellent dissolving ability of formic acid on biological matrices, it has never been applied for the isolation of NPs from biota.

Mercury (Hg) occupies the third position in the substance priority list established by the agency for toxic substances and disease registry (ATSDR) and is considered one of the top ten chemicals of major public health concern by the World Health Organization (WHO). Despite its unquestionable toxicity, the mechanisms of metabolization and fate in living organisms remain unclear. Tiemannite (HgSe) is considered the end-product of Hg detoxification mechanisms in vertebrates [34–37]. This solid compound has been identified in human brain [37], fish [38,39], marine mammal [34,40] and more recently, in eagles [23] and seabird tissues [35]. There is an unquestionable growing interest on the size, concentration [12,23,34,35,39,41] and isotopic [42–44] characterization of HgSe NPs in living organisms, in order to better understand Hg metabolism and HgSe NPs formation.

The current work explores the potential of formic acid for HgSe NPs isolation from animal tissue samples and compares it with enzymatic based sample treatment. A set of samples including various internal tissues of giant petrels (*Macronectes* sp.) was used on this study. This seabird species exhibits particularly high Hg and selenium (Se) levels reaching values over 1000 μg g^{-1} dry weight (dw) for both elements in the liver [35,43], as a consequence of their elevated trophic position and long-life span [45]. The combination of formic acid sample treatment methodology with spICP-MS measurements offers a fast and simple methodology to perform screening and quantification of HgSe NPs in complex matrices such as biological tissues.

2. Materials and methods

2.1. Reagents and standards

All reagents used were of analytical grade. HgSe NPs standard (PURATREM $\gamma = 99.99\%$ Hg) was obtained from Strem chemicals and used without any further purification. Working standard solutions of arsenic (As), cadmium (Cd), Hg and Se, were prepared daily by appropriate dilution of the stock standard solutions (Sigma Aldrich) in water using ultrapure water (>18 MΩ cm) obtained from a Milli-Q system (Millipore, Bedford, MA, USA) and stored at 4 °C before use. A standard reference gold nanoparticle (AuNPs) solution was daily prepared by diluting 30 nm citrate-AuNPs reference material (LGC5050) to reach a concentration level of 7.5 ng L^{-1} (2.5×10^7 particle L^{-1}).

2.2. Samples description

The giant petrels seabirds were collected freshly after their death near to the scientific platforms in the Kerguelen archipelago (Southern Indian Ocean) and Adelie Land (Antarctic continent) in 2014. Liver, kidneys, muscle, brain, feathers and blood were collected during the necropsy. After dissection, all the samples were stored at −20 °C in individual plastic bags until being processed in the laboratory.

2.3. HgSe NPs extraction procedures: enzymatic and formic acid-based sample treatment

Two different methods were applied in order to isolate the HgSe NPs from seabird samples: a formic acid (*i*) and an enzymatic (*ii*) based sample treatment. For both treatments, approximately 25 mg of homogenised and freeze-dried sample was defatted by shaking with 3 mL MeOH (Sigma-aldrich, HPLC grade ≥99.9%) for 5 min, centrifugation at 14000Xg during 12 min, and removal of MeOH. For the first treatment (i), 5 mL of 50 = 50% formic acid (Scharlauφ = 98–100%, reagent grade) was added and the mixture was kept at 85 °C for 2 h in a hot-block [46]. The enzymatic treatment (*ii*) was based on the approach proposed by Loeschner et al. [25] with slight modifications. In brief, 3 mL of a solution containing 2 mg mL^{-1} protease K (Sigma-Aldrich) in 50 mM ammonium bicarbonate (Sigma-Aldrich) buffer (pH 7.4) were added to the defatted sample and ultrasonicated with ultrasonication probe (USP) during 2 min at the applied amplitude of 21% (100 W). Sonication was performed in pulse mode to avoid overheating (which was also reduced by immersing the flask in ice). The ultrasound probe was immersed 1 cm and these conditions were kept constant for all the extractions. Then, 2 mL of γ = 4% sodium dodecyl sulfate (SDS, Sigma-Aldrich) in 50 mmol L^{-1} ammonium bicarbonate buffer (pH 7.4) were added to the resulting solution and ultrasonicated in a bath for 1 h.

The resulting extracts from both treatments (*i* and *ii*) were centrifuged by using cut-off filters of 50 kDa [34] at 140,000 g during 5 min in an ultracentrifuge HimaCs 120GX model (Hitachi, Tokyo, Japan). The filter was abundantly washed with Milli-Q water until total removal of soluble Hg and Se [34]. To recover the concentrated NPs, the cut-off filter device was inverted in a clean microcentrifuge tube and centrifuge for 2 min at 1000×*g*, as suggested by the filter manufacturer.

2.4. Single-particle Inductively Coupled Plasma Mass Spectrometry (spICP-MS) analysis and data processing

HgSe NPs isolated from giant petrel internal tissues (liver, kidneys, muscle, and brain) were characterised in terms of composition, size distribution and particle number concentration by Inductively Coupled Plasma Mass Spectrometry (ICP-MS) operating in single particle mode (spICP-MS). An Agilent 7700x ICP-MS equipped with a MicroMist nebulizer and Scotttype spray chamber was used for data acquisition which were collected in the time-resolved analysis (TRA) mode, using a dwell time of 3 ms and an acquisition time of 60 s (20000 points). Hg and Se were measured for single particle analysis in separate runs. The limit of detection in size was 30 nm and 46 nm for Se and Hg, respectively calculated following the indications given by Laborda *et* al. 2020 [47]. As and Cd were also monitored separately. Operating conditions are listed in Table S1.

Transport efficiency was determined daily through the particle frequency method [48] using AuNPs standard solution prepared by diluting 30 nm citrate-AuNPs reference material LGC5050 until a concentration of 7.5 ng L^{-1} was reached. The sample uptake rate was also checked daily in triplicate by weighting a vial containing Milli-Q water before and after 2 min of aspiration, and was found to be constantly around 0.3 ml min^{-1}. Calibration curve of ionic Hg and Se was prepared daily within the 1–100 ng L^{-1} range and by employing a Hg and Se standard solution for ICP-MS (Sigma Aldrich). Samples were diluted with Milli-Q water before spICP-MS measurements with a dilution factor ranging from 10 to 500 depending on the background level.

Raw signal intensity data were processed manually using a dedicated spreadsheet developed by the National Institute of Food Safety in the Netherlands (RIKILT) from which particle number concentration and particle mass concentration were calculated. Particles were discriminated from the background signal using a 5σ approach [47]. Particle size diameter and the corresponding size histogram were obtained from the density of HgSe, the mass fraction of Hg/HgSe and Se/HgSe and by assuming a spherical shape of the nanoparticles.

2.5. Transmission Electron Microscopy (TEM)

HgSe NPs isolated from giant petrel tissues were also characterised in terms of size, morphology and composition by using TEM (JEOL JEM 1400; USA) equipped with an Energy Dispersive X-ray Spectroscopy (EDXS) composition system (Oxford Inca). Samples were dropped onto copper grids and dried in clean air. TEM measurements were performed at an accelerating voltage of 200 kV.

2.6. Statistical analysis

Statistically significant differences between groups were determined by a two-way analysis of variance (ANOVA) and by using Statgraphics v19 software (Manugistics, Rockville, USA). Values are considered significantly different if $p < 0.05$.

3. Results and discussion

3.1. Evaluation of the effect of reagents and extraction procedure on HgSe nanoparticles standards

Two different approaches were applied on the isolation of HgSe NPs from giant petrel tissues. One of them, based on the conventional use of enzymes (precisely Protease K) and the other one, exploring for the first time the potential of formic acid on NPs extraction (Table 1).

The first step to evaluate the performance of these extraction procedures is to test the effect of different reagents on HgSe NPs stability. For this purpose, a HgSe NPs standard was dispersed separately in φ = 50% formic acid; 2 mg mL^{-1} protease K in 50 mmol L^{-1} ammonium bicarbonate buffer (pH 7.4); γ = 4% SDS in a 50 mmol L^{-1} ammonium bicarbonate buffer (pH 7.4) and finally Milli-Q water, as a control. The resulting dispersions were characterised by TEM (Fig. 1a–d). Fig. 1a shows aggregated nanoparticles with polygonal shapes and curved ends between 10 and 50 nm, which correspond with HgSe NPs standard in water media. However, they seem to be dispersed by the action of media employed for extraction procedures in smaller submicronsized agglomerates of particles (Fig. 1b, c, and 1d), but composed of small particles with the same size than those observed in the control sample (Fig. 1a). No significant difference in the size and morphology of the aggregates was observed among the treatment employed. Moreover, the spectrum (Fig. 1e) obtained by Energy-Dispersive X-ray (EDXS) spectroscopy confirms the presence of Hg and Se in the nanoparticles analysed.

According to this preliminary test, it could be concluded that the reagents used at the different sample treatment steps (φ = 50% formic acid, 2 mg mL^{-1} protease K in 50 mmol L^{-1} ammonium bicarbonate buffer (pH 7.4) and γ = 4% SDS in a 50 mmol L^{-1} ammonium bicarbonate buffer (pH 7.4)) did not produce any effect on nanoparticle integrity, size or agglomerated state. Therefore, both extraction procedures might be potentially suitable for the isolation of HgSe NPs from biological tissues.

Afterwards, spICP-MS was employed to characterize the effect of the extraction procedures on the size of HgSe NPs. For this purpose, HgSe NPs standard was submitted to both extraction methods before analysis.

The accuracy of the spICP-MS measurements was evaluated by means of using gold nanoparticles reference material LGC5050 since no reference material for HgSe NPs is commercially available. Therefore, particle mean size and distribution, as well as particle number concentration were determined in three individuals AuNPs LGC5050 suspensions. No statistical differences ($p < 0.05$) were observed among values determined by spICP-MS and those certified (data shown in SI). Moreover, these measurements were repeated several times on different days and provided similar results.

Furthermore, mean size, size distribution and particle number concentration of HgSe NPs were calculated by employing RIKILT spread sheet [49] after performing spICP-MS measurements. As simultaneous

Table 1
Compilation of extraction and characterization methods used for HgSe in biological samples.

Treatment	Reagent	Extraction procedures	Time incubation/extraction	Characterization techniques	Matrix	Ref
Basic	TMAH	samples mixed with φ = 20% TMAH solution	For 12 h at room temperature after sonicating for 1 h	spICP-MS	Liver and muscle of cetaceans	[12]
Enzyme	Pancreatin + lipase	0.5 g of sample mixed with 7 mL enzyme solution (3.0 mg L^{-1} pancreatin, 3.0 g L^{-1} lipase, 0.2 M NaH_2PO_4, and 0.2 M NaOH; pH 7.4)	Placed in ice-cooled sonication bath for 10 min then at 37 °C for 1 h	spICP-MS	Seafood	[39]
	Protease + SDS	0.02 g sample + 1 mg mL^{-1} protease + 5 mg mL^{-1} SDS in 50 mM ammonium carbonate buffer (pH 7.4)	Overnight at 37 °C		Liver of raptors Liver and brain of pilot whales	[23] [34]
	Protease + SDS	0.02 g sample + 3 mL (2 mg mL^{-1} protease K in 50 mM ammonium bicarbonate pH 7.4) USP then + 2 mL of γ = 4% SDS in 50 mmol L^{-1} ammonium bicarbonate buffer (pH 7.4)	-USP during 2 min at 21% (before SDS) -Ultrasonication in an ultrasound bath at room temperature for 1 h (after SDS)	spICP-MS	Giant petrel tissues	This study
Acid	Formic acid	0.02 g sample + 5 mL of φ = 50% formic acid	85 °C for 2 h	spICP-MS	Giant petrel tissues	This study

detection of Hg and Se in the particles isolated was not possible due to the fact that a quadrupole ICP-MS system was employed for the analyses, calculations of nanoparticles parameter were based on separate measurements monitoring either Hg or Se[34].

HgSe NPs mean diameter of the standard submitted to enzymatic extraction was 213 ± 98 and 217 ± 91 nm for Hg and Se, respectively. Similar results were obtained for the formic acid extraction procedure, with a mean diameter of 210 ± 98 and 175 ± 77 nm for Hg and Se, respectively. No significant difference (p_{ANOVA} <0.05) was found when the mean diameter of the standard HgSe NPs dispersed in water was compared to that obtained after submitted the standard to the enzymatic and formic acid extraction procedures. These results were consistent with the data obtained by TEM described above.

3.2. *Characterization of HgSe nanoparticles isolated from giant petrel tissues by spICP-MS and TEM*

Once it has been verified that enzymatic and formic acid extraction did not affect HgSe NPs (standard) size, shape or agglomerate state, both extraction methods were applied in different tissues of giant petrels (liver, kidneys, muscle and brain) following the procedure described in 2.3. The isolated NPs were characterised in terms of size, size distribution and nanoparticle number concentration (part L^{-1}).

Fig. 2 shows a typical time scan for Se (2a) and Hg (2b) obtained by spICP-MS analyses of HgSe NPs isolated from giant petrel tissues with formic acid. In both, Hg and Se scans, several pulses above the background signal with a high variability in signal intensity were detected indicating the formation of large particles likely due to particle aggregation. This fact was confirmed by TEM analyses. Fig. 2c shows a micrograph which correspond to HgSe NPs isolated from the kidney after formic acid extraction. Aggregated nanoparticles between 10 and 60 nm with polygonal shapes and curved ends constituting larger crystals of micron orders as Hg–Se clusters could be observed. The aggregate size is in agreement with a recent study in internal tissues of giant petrels where they found HgSe aggregate in liver, kidneys, muscle and brain (5–100 nm) with electron microscopy [35]. Moreover, EDXS analyses (Fig. 2d) also confirms the presence of Se and Hg as well as As and Cd. The occurrence of As and Cd will be discussed in section 3.3. On the other hand, Cu signal in EDXS spectrum come from the copper grids used for sample preparation in TEM.

As previously mentioned, simultaneous detection of Hg and Se by spICP-MS in the isolated particles was not possible. Therefore, calculations of nanoparticles parameter were based on separate measurements monitoring either Hg or Se in a set of nanoparticles isolated from eight different samples (various tissues) obtained by the extraction procedures using formic acid or enzymatic treatment.

Size distribution histograms are shown in Fig. S1 (Se) and S2 (Hg). In both cases, histogram profiles clearly demonstrated the variability of the particle dimensions which also leads to particle aggregation and formation of large clusters, as can be shown in Fig. 2e. This variability could be also appreciated in the standard deviation values that follow the mean size of HgSe NPs gathered in Table 2. Results corresponding to organs of other three individuals are compiled in Table S2.

Moreover, data from Table 2 indicated that the size of isolated HgSe NPs using both extraction methods are comparable in all the giant petrel tissues. On the other hand, statistical analyses evidenced significant differences (P_{ANOVA} <0.05) among values related with particle number concentration obtained after enzymatic procedure and soft acidic digestion method with formic acid in all the tissues analysed (Table 2). However, both values, those obtained with the enzymatic procedure and those obtained with soft acid digestion, are in the same order of magnitude (Table 2). Although the soft acidic digestion extracts smaller number of particles, it has numerous advantages that may compensate this tiny difference. Some of the main advantages of using formic acid for HgSe NPs isolation (Table 2) are the reduced number of steps in the extraction procedure, which lead to a better cost effective method. In addition, the formic acid extraction involves a single reagent, which is considered relatively green solvent [29,50].

In general, the HgSe size values found in this set of giant petrel tissues (Table 2) are in agreement with those reported in liver and brain of pilot whales [34]. In the mentioned tissues of the marine mammals, the spICP-MS analyses revealed the presence of particles up to 500 nm. The authors pointed out that the biologically formed HgSe nanoparticles act as nucleation centres for the formation of large Se–Hg clusters, which grow with the age of the animals. The reported differences between particle sizes of HgSe NPs found in pilot whale tissues (range 160–538 nm) were related to aggregation of particles and formation of large clusters after MeHg demethylation and deposition in the form of HgSe aggregates as a final product of detoxification [34].

In this study, the NPs isolated from seabirds tissues shows a great variability in particle dimensions (Table 2, Figs. S1 and S2). In the kidneys, TEM images brought the evidence of presence of Hg–Se clusters which might be formed from smaller primary HgSe nanoparticles between 10 and 60 nm (Fig. 2c), as previously reported in whales [34]. A recent study in giant petrels also described the presence of sparsely distributed electron-dense aggregates of 5 nm up to 100 nm HgSe nanocrystals imaged with TEM from liver, kidneys and muscle [35].

It is likely that Hg–Se clusters could be dispersed in smaller aggregates during spICP-MS and thus we detected them as HgSe particles between 100 and 250 nm (Table 2). Recently, in cetaceans liver and muscle, HgSe characterization by spICP-MS revealed the presence of HgNPs with a diameter size between 150-300 nm and 100–200 nm

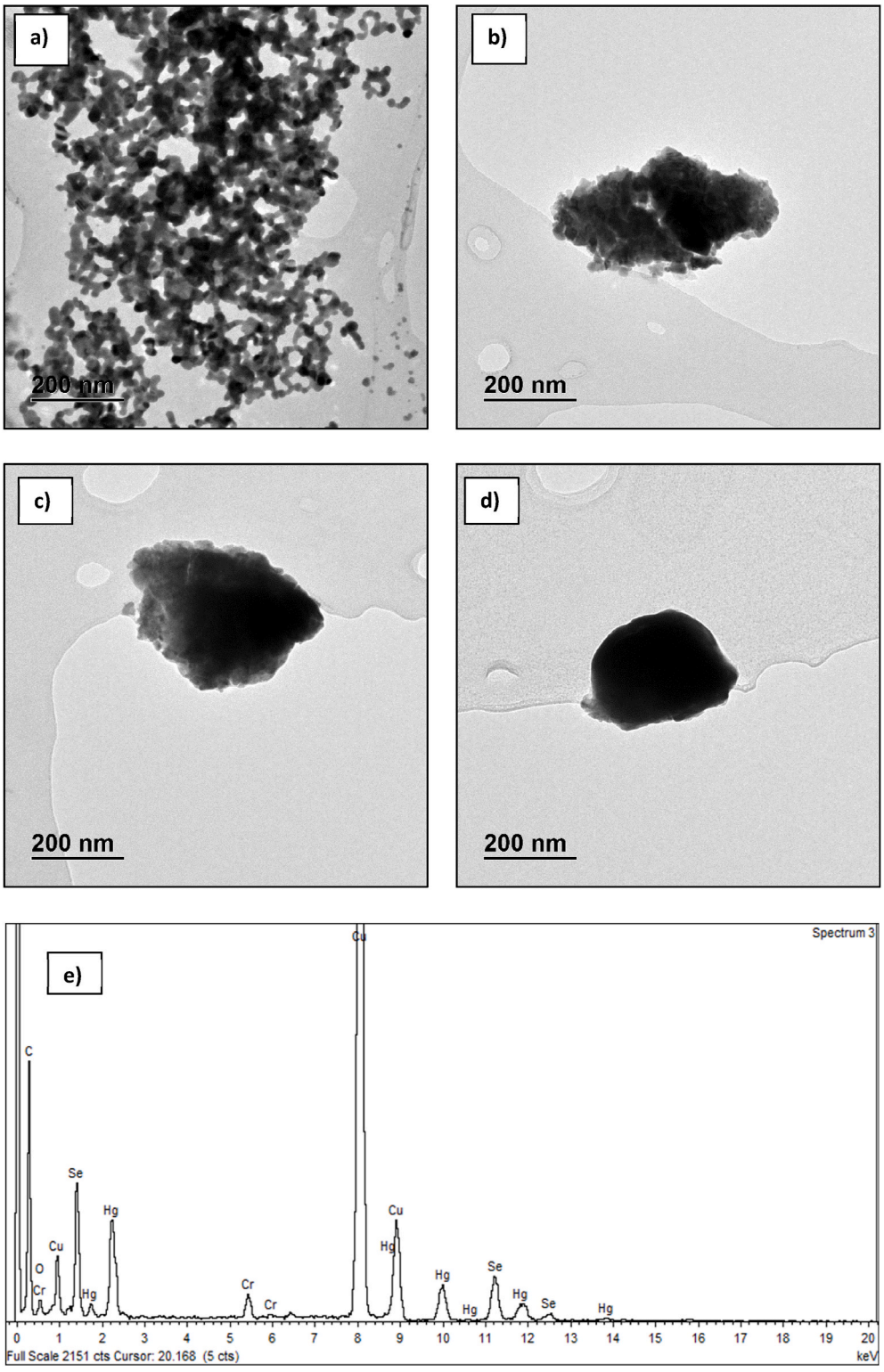

Fig. 1. TEM images of the HgSe NPs standard dispersed in: (a) Milli-Q water, (b) φ = 50% formic acid, (c) 2 mg mL^{-1} protease K in 50 mmol L^{-1} ammonium bicarbonate buffer (pH 7.4) (d) γ = 4% SDS in a 50 mmol L^{-1} ammonium bicarbonate buffer (pH 7.4) (e) EDXS of the HgSe NPs standard dispersed in Mili-Q water.

respectively, with SeNPs diameter size larger than 100 nm [12]. In this sense, another study reported the presence of HgSe as micro or nanoparticles in the liver of golden eagle (*Aquila chrysaetos*), with spICP-MS analysis, HgNPs were identified with a mean diameter <18–43 nm [23].

The reduced number of samples characterized (Table 2) in the current study hamper the identification of trends regarding the size and/or concentration variation with age and/or Hg and Se concentrations.

3.2.1. *Ultrasound probe sonication assistance for HgSe nanoparticles isolation*

Enzymatic treatments have been conventionally employed for NPs isolation from biological samples of animal origin [51]. Recently, ultrasound assistance in enzymatic extractions has proven to be effective in reducing the extraction time, without affecting the initial characteristics of the NPs [15,19]. USP, which is widely used on the extraction of

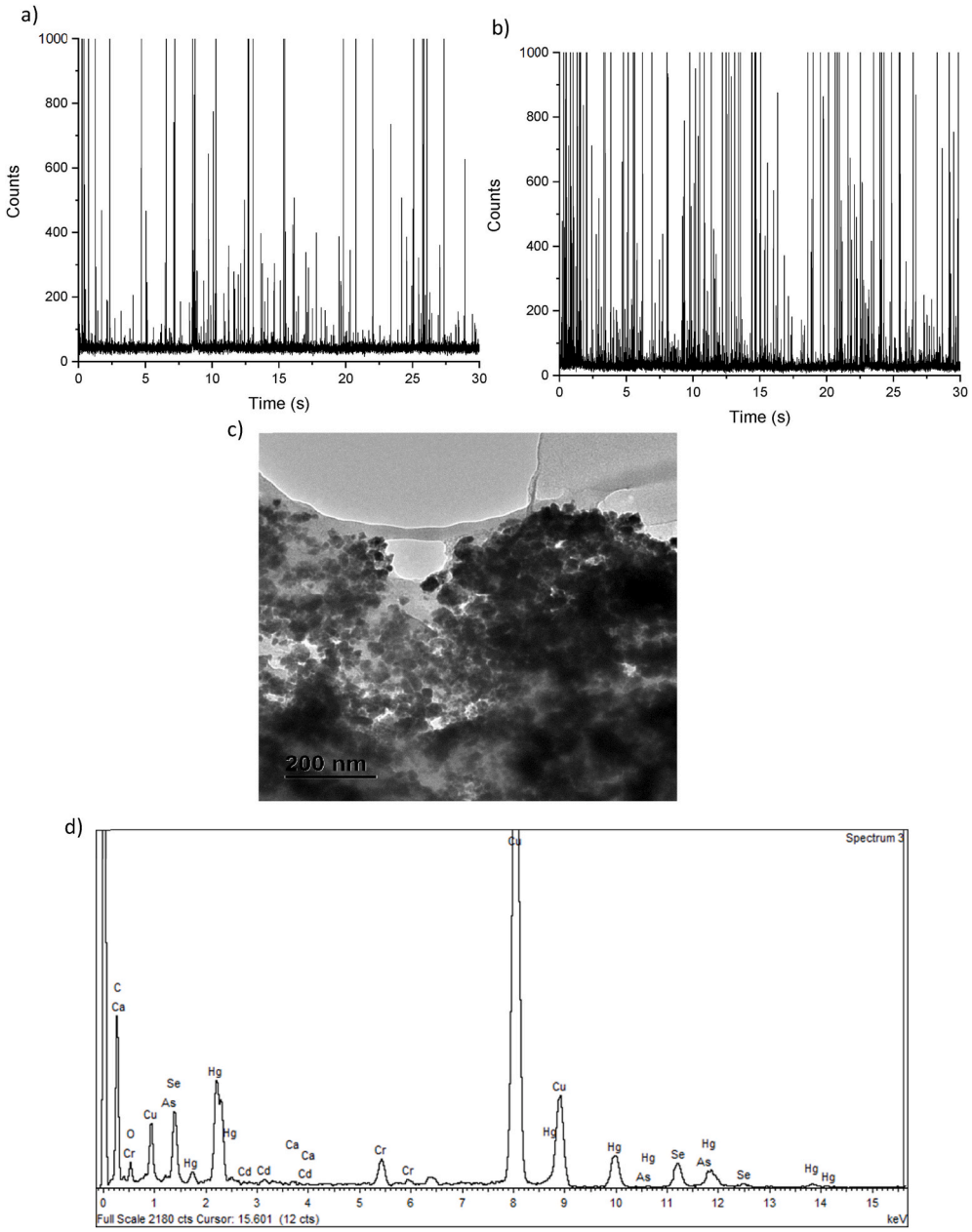

Fig. 2. Time resolved spICP-MS analyses of ^{78}Se (a) and ^{202}Hg (b) from HgSe NPs isolated from liver; and TEM image (c) and EDXS (d) analysis of HgSe NPs isolated from the kidney of giant petrels from the Southern Ocean.

Table 2
Concentrations of Hg and Se in μg g^{-1} (dry weight), % MeHg and Se:Hg molar ratio [43] with the results of spICP-MS analysis, showing the mean size (nm) of the detected particles and particle concentration (NPs kg^{-1}) individually for Hg and Se in the different internal tissues of giant petrel (n = 3).

Matrix	Hg (μg g^{-1})	Se (μg g^{-1})	MeHg (%)	Se:Hg	Extraction	HgNPs		SeNPs	
						Size (nm)	NPC (NPs kg^{-1})	Size (nm)	NPC (NPs kg^{-1})
Liver	381.69 ± 6.56[a]	222.17 ± 26.59[b]	5.80 ± 0.11[b]	1[b]	Formic Acid	215 ± 90	(7.1 ± 0.1) x 10^{9}	176 ± 72	(2.2 ± 0.2) x 10^{9}
					Enzymatic	148 ± 58	(4.2 ± 0.1) x 10^{9}	204 ± 91	(1.9 ± 0.1) x 10^{9}
Kidneys	50.84 ± 0.67[a]	131.09 ± 10.33[b]	33.90 ± 0.50[b]	7[b]	Formic Acid	142 ± 66	(8.9 ± 1.5) x 10^{7}	122 ± 46	(1.7 ± 0.4) x 10^{8}
					Enzymatic	151 ± 91	(5.8 ± 0.7) x 10^{9}	158 ± 53	(1.7 ± 0.2) x 10^{9}
Muscle	29.18 ± 0.32[a]	31.37 ± 2.80[b]	36.72 ± 0.66[b]	3[b]	Formic Acid	184 ± 72	(2.0 ± 0.6) x 10^{11}	168 ± 45	(3.0 ± 0.1) x 10^{10}
					Enzymatic	137 ± 57	(3.9 ± 0.1) x 10^{9}	173 ± 47	(2.6 ± 0.2) x 10^{9}
Brain	3.23 ± 0.22[a]	47 ± 4.33	33.54 ± 0.95[b]	10	Formic Acid	171 ± 71	(4.1 ± 0.3) x 10^{9}	169 ± 46	(3.2 ± 0.2) x 10^{9}
					Enzymatic	192 ± 66	(9.8 ± 0.2) x 10^{9}	158 ± 43	(1.9 ± 0.1) x 10^{9}

[a] Values reported elsewhere (Renedo et al., 2021) [45].
[b] Values reported elsewhere (Queipo et al., 2022) [43].

organometallic species [15], has been proposed to assist enzymatic hydrolysis for NPs isolation from biological samples. This strategy allowed a reduction of the pancreatin and lipase incubation time, from overnight incubation by using conventional enzymatic extractions to a faster procedure (i.e., 10 min) [19]. The described method was successfully applied on the isolation of Ag NPs [19] and TiO_2 NPs [52] before spICP-MS analyses, from a variety of bivalve molluscs, including clams, cockles, mussels, razor clams, oysters and variegated scallops.

The efficiency of enzymatic probe sonication approaches for both Hg and Se water soluble species from biological samples is conclusive. The mentioned approach allows miniaturizing extraction of Hg species from zebrafish embryos [53] (2 mg) and selenocysteine ($SeCys_2$), methylselenocysteine (MeSeCys), selenate (Se (IV)), selenomethionine (SeMet) and selenite (Se (VI)) from animal feeds [54,55]. However, USP had not been exploited so far for HgSe NPs isolation. The current work revealed for the first time the potential of enzymatic probe sonication for HgSe NPs isolation from a variety of animal samples, which results in a reduction of enzymatic incubation time of 12 h (classical procedure) to a few minutes (Table 2).

3.3. Presence of As and Cd in the isolated nanoparticles

EDXS analyses (Fig. 2d) reveals the presence of As and Cd in the isolated fraction containing HgSe NPs. Considering this result, both elements were monitored by spICP-MS in different tissues of giant petrels (liver, kidneys, muscle and brain). Pulses above the background signal were only detected for Cd in liver and muscle samples (Fig. 3a and b, respectively). However, since the number of events were not enough for being statistically significant, further conclusion about the exact composition or calculations of size distribution or particle concentration could not be drawn. The occurrence of As and Cd in the isolated HgSe NPs fraction is consistent with the recent report of Hg NPs principally complexed with Se and S, but also with Ag, Cd, and Pb in cetaceans [12]. In liver and muscles a of these marine mammals, Ag, Cd, and Pb were found combined to Hg NPs at both small (5–40 nm) and large size (>100 nm) [12].

The simultaneous Cd and Se exposure of nematodes (*Caenorhabditis elegans*) leads to the formation CdSe/CdS nanoparticles, which were continuously excreted from the body, benefitting survival [56]. The studies of Cd-containing NPs in marine animals is still scarce. The occurrence of Cd-containing granules in kidneys from white side-dolphins (*Lagenorhyncus acutus*) has been reported as a potential detoxification mechanism [57]. Meanwhile, in pilot whales, Cd accumulates linearly in liver, exhibiting a positive correlation with Se. Such correlation has been attributed by the authors of the study to possible similarities in the metabolic pathways of these elements. The formation of Cd/Se complexes has been related with Cd detoxification processes [56,58]. However, the mechanisms of formation of such complexes remains unknown. Regarding As, after the co-administration of As, Hg and Se, As–Se and Hg–Se compounds was found formed in the bloodstream of rabbits [59].

To our knowledge, the present study is the first to report the possible occurrence of Cd particles and As particles associated with HgSe NPs in seabirds. This finding supports the hypothesis that the formation of micro-or nanoparticles is a detoxification mechanism not exclusive of Hg. The occurrence of As and Cd in this specific fraction should be considered a preliminary results due to the reduced number of individuals investigated and claim for the characterization in larger set of samples. The understanding of these (detoxification) mechanisms claims for the development of new analytical strategies and the combination of microscope images [12,23,34,35] and stable isotopic analyses [43] in a larger set of animals and tissues.

4. Conclusions

In summary, the present work demonstrates the successful application of both enzymatic probe sonication and formic acid on HgSe isolation from animal samples. The ultrasonic assistance of the classical enzymatic procedure was for the first time applied on HgSe NPs isolation, leading to a time reduction from 12 h to 2 min. On the other hand, the formic acid extraction proposed presents several advantages in comparison to the most conventional (enzymatic) treatments. The use of this organic acid guarantees a simple, cost-effective and green procedure for HgSe NPs extraction from biological samples and open new perspectives for its application to other metallic NPs. Indeed, the combination of formic acid sample treatment methodology with spICP-MS and TEM measurements allowed us to identify the possible occurrence of Cd particles and As particles associated with HgSe NPs in seabirds.

Author contributions

KH and BGG: conceptualization, investigation, data curation, formal analyses, writing-original draft, writing-review&editing; ZP: conceptualization, funding acquisition, investigation, supervision, writing-review&editing; PB and YC: investigation, supervision, writing-review&editing. DA: investigation, supervision, resources, writing-review&editing; YM: conceptualization, investigation, sources, supervision, writing-review&editing.

Declaration of competing interest

The authors declare that they have no known competing financial interests or personal relationships that could have appeared to influence the work reported in this paper.

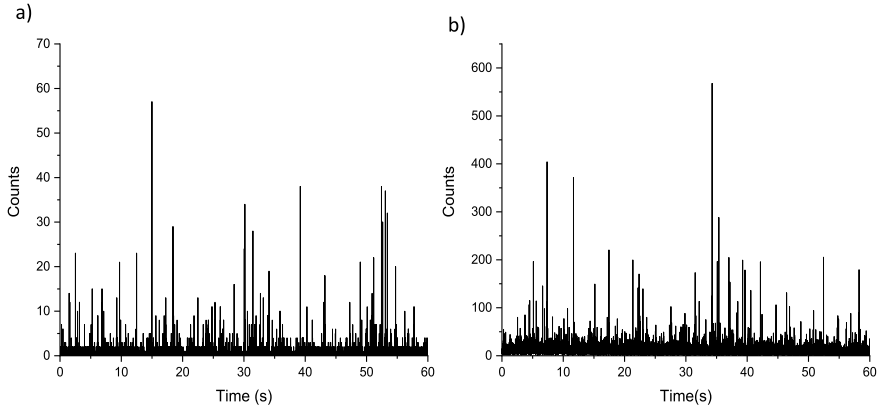

Fig. 3. Time resolved spICP-MS analyses of ^{111}Cd from particles isolated from liver (a) and muscle (b).

Data availability

Data will be made available on request.

Acknowledgements

The authors thank the Agence Nationale de la Recherche (MERSEL Project No. ANR-18-CE34-0004-01), CNRS (MITI-ISOISEAUX) and the Communauté d'Agglomération Pau Béarn Pyrénées (MERISOTOP) for funding. This project has also received funding from the European Union's Horizon 2020 research and innovation programme under the Marie Skłodowska-Curie grant agreement No 101007962". Support was provided to Yves Cherel by the Institut Polaire Français Paul Emile Victor (IPEV programme no. 109, C. Barbraud) and the Terres Australes et Antarctiques Francaises, and to Paco Bustamante by the Institut Universitaire de France (IUF). The authors would like to acknowledge PS Analytical for their instrumental and technical support. K. El Hanafi acknowledges the international mobility grant from the UPPA doctoral school. UCM group thanks to the Community of Madrid (PB2018/BAA-4393, AVANSECAL II-CM) and the Spanish Ministry of Science, Innovation and Universities (PID2020-114714RB-IOO) for funding.

Appendix A. Supplementary data

Supplementary data to this article can be found online at https://doi.org/10.1016/j.aca.2023.340952.

References

[1] S. Sudheer, R.G. Bai, K. Muthoosamy, R. Tuvikene, V.K. Gupta, S. Manickam, Biosustainable production of nanoparticles via mycogenesis for biotechnological applications: a critical review, Environ. Res. 204 (2021), 111963.
[2] S. Srivastava, Z. Usmani, A.G. Atanasov, V.K. Singh, N.P. Singh, A.M. Abdel-Azeem, R. Prasad, G. Gupta, M. Sharma, A. Bhargava, Biological nanofactories: using living forms for metal nanoparticle synthesis, Mini Rev. Med. Chem. 21 (2021) 245–265.
[3] L. Wang, J. Zhao, L. Cui, Y.-F. Li, B. Li, C. Chen, Comparative nanometallomics as a new tool for nanosafety evaluation, Metallomics 13 (2021), mfab013.
[4] C. Chen, D.T. Leong, I. Lynch, Rethinking nanosafety: harnessing progress and driving innovation, Small 16 (2020), 2002503.
[5] A. Nemmar, P.M. Hoet, B. Vanquickenborne, D. Dinsdale, M. Thomeer, M. F. Hoylaerts, H. Vanbilloen, L. Mortelmans, B. Nemery, Passage of inhaled particles into the blood circulation in humans, Circulation 105 (2002) 411–414.
[6] G. Oberdörster, Z. Sharp, V. Atudorei, A. Elder, R. Gelein, A. Lunts, W. Kreyling, C. Cox, Extrapulmonary translocation of ultrafine carbon particles following whole-body inhalation exposure of rats, J. Toxicol. Environ. Health A 65 (2002) 1531–1543.
[7] D. Di Bella, J.P. Ferreira, O.S. Renee de Nazare, C. Echem, A. Milan, E.H. Akamine, M.H. Carvalho, S.F. Rodrigues, Gold nanoparticles reduce inflammation in cerebral microvessels of mice with sepsis, J. Nanobiotechnol. 19 (2021) 1–15.
[8] I. Ozcicek, N. Aysit, C. Cakici, A. Aydeger, The effects of surface functionality and size of gold nanoparticles on neuronal toxicity, apoptosis, ROS production and cellular/suborgan biodistribution, Mater. Sci. Eng. C 128 (2021), 112308.
[9] S. Zhou, X. Li, M. Zhu, H. Yu, R. Chu, W. Chen, B. Wang, M. Wang, L. Zheng, Z. Chai, Hepatic impacts of gold nanoparticles with different surface coatings as revealed by assessing the hepatic drug-metabolizing enzyme and lipid homeostasis in mice, NanoImpact 20 (2020), 100259.
[10] S. Naasz, R. Altenburger, D. Kühnel, Environmental mixtures of nanomaterials and chemicals: the Trojan-horse phenomenon and its relevance for ecotoxicity, Sci. Total Environ. 635 (2018) 1170–1181.
[11] M. Popescu, A. Velea, A. Lőrinczi, Biogenic production of nanoparticles, Dig. J. Nanomater. Biostructures DJNB 5 (2010) 1035–1040.
[12] X. Ji, L. Yang, F. Wu, L. Yao, B. Yu, X. Liu, Y. Yin, L. Hu, G. Qu, J. Fu, Identification of mercury-containing nanoparticles in the liver and muscle of cetaceans, J. Hazard Mater. 424 (2022), 127759.
[13] S. Lopez-Sanz, F.J.G. Bernardo, R.C.R. Martín-Doimeadios, A. Rios, Analytical metrology for nanomaterials: present achievements and future challenges, Anal. Chim. Acta 1059 (2019) 1–15.
[14] M.S. Jimenez, M.T. Gomez, E. Bolea, F. Laborda, J. Castillo, An approach to the natural and engineered nanoparticles analysis in the environment by inductively coupled plasma mass spectrometry, Int. J. Mass Spectrom. 307 (2011) 99–104.
[15] J.J. López-Mayán, S. del-Angel-Monroy, E. Pena-Vazquez, M.C. Barciela-Alonso, P. Bermejo-Barrera, A. Moreda-Pineiro, Titanium dioxide nanoparticles assessment in seaweeds by single particle inductively coupled plasma–Mass spectrometry, Talanta 236 (2022), 122856.
[16] L. Cid-Barrio, D. Bouzas-Ramos, A. Salinas-Castillo, Y. Ogra, J.R. Encinar, J. M. Costa-Fernández, Quantitative assessment of cellular uptake and differential toxic effects of HgSe nanoparticles in human cells, J. Anal. At. Spectrom. 35 (2020) 1979–1988.
[17] F.A. Monikh, L. Chupani, D. Arenas-Lago, Z. Guo, P. Zhang, G.K. Darbha, E. Valsami-Jones, I. Lynch, M.G. Vijver, P.M. van Bodegom, Particle number-based trophic transfer of gold nanomaterials in an aquatic food chain, Nat. Commun. 12 (2021) 1–12.
[18] X. Wang, S. Hong, H. Lian, X. Zhan, M. Cheng, Z. Huang, M. Manzo, L. Cai, A. Nadda, Q. Van Le, Photocatalytic degradation of surface-coated tourmaline-titanium dioxide for self-cleaning of formaldehyde emitted from furniture, J. Hazard Mater. 420 (2021), 126565.
[19] M.V. Taboada-López, N. Alonso-Seijo, P. Herbello-Hermelo, P. Bermejo-Barrera, A. Moreda-Pineiro, Determination and characterization of silver nanoparticles in bivalve molluscs by ultrasound assisted enzymatic hydrolysis and sp-ICP-MS, Microchem. J. 148 (2019) 652–660.
[20] I. De la Calle, M. Menta, F. Séby, Current trends and challenges in sample preparation for metallic nanoparticles analysis in daily products and environmental samples: a review, Spectrochim. Acta Part B At. Spectrosc. 125 (2016) 66–96.
[21] C.-K. Su, Y.-C. Sun, Considerations of inductively coupled plasma mass spectrometry techniques for characterizing the dissolution of metal-based nanomaterials in biological tissues, J. Anal. At. Spectrom. 30 (2015) 1689–1705.
[22] I. Abad-Alvaro, D. Leite, D. Bartczak, S. Cuello-Nunez, B. Gomez-Gomez, Y. Madrid, M. Aramendia, M. Resano, H. Goenaga-Infante, An insight into the determination of size and number concentration of silver nanoparticles in blood using single particle ICP-MS (spICP-MS): feasibility of application to samples relevant to in vivo toxicology studies, J. Anal. At. Spectrom. 36 (2021) 1180–1192.
[23] S.T. Lancaster, G. Peniche, A. Alzahrani, M. Blanz, J. Newton, M.A. Taggart, W. T. Corns, E.M. Krupp, J. Feldmann, Mercury speciation in Scottish raptors reveals high proportions of inorganic mercury in Scottish golden eagles (Aquila chrysaetos): potential occurrence of mercury selenide nanoparticles, Sci. Total Environ. 829 (2022), 154557.
[24] K. Loeschner, M.S.J. Brabrand, J.J. Sloth, E.H. Larsen, Use of alkaline or enzymatic sample pretreatment prior to characterization of gold nanoparticles in animal tissue by single-particle ICPMS, Anal. Bioanal. Chem. 406 (2014) 3845–3851.
[25] K. Loeschner, J. Navratilova, C. Købler, K. Mølhave, S. Wagner, F. von der Kammer, E.H. Larsen, Detection and characterization of silver nanoparticles in chicken meat by asymmetric flow field flow fractionation with detection by conventional or single particle ICP-MS, Anal. Bioanal. Chem. 405 (2013) 8185–8195.
[26] B. Gomez-Gomez, M.T. Perez-Corona, Y. Madrid, Using single-particle ICP-MS for unravelling the effect of type of food on the physicochemical properties and gastrointestinal stability of ZnONPs released from packaging materials, Anal. Chim. Acta 1100 (2020) 12–21.
[27] S. Elzey, V.H. Grassian, Agglomeration, isolation and dissolution of commercially manufactured silver nanoparticles in aqueous environments, J. Nanoparticle Res. 12 (2010) 1945–1958.
[28] Z. Arslan, M. Ates, W. McDuffy, M.S. Agachan, I.O. Farah, W.W. Yu, A.J. Bednar, Probing metabolic stability of CdSe nanoparticles: alkaline extraction of free cadmium from liver and kidney samples of rats exposed to CdSe nanoparticles, J. Hazard Mater. 192 (2011) 192–199.
[29] L. Tormen, R.A. Gil, V.L. Frescura, L.D. Martinez, A.J. Curtius, Determination of trace elements in biological samples treated with formic acid by inductively coupled plasma mass spectrometry using a microconcentric nebulizer, Spectrochim. Acta Part B At. Spectrosc. 65 (2010) 959–966.
[30] M. Kan, S.N. Willie, C. Scriver, R.E. Sturgeon, Determination of total mercury in biological samples using flow injection CVAAS following tissue solubilization in formic acid, Talanta 68 (2006) 1259–1263.
[31] E. Alonso-Rodríguez, J. Moreda-Piñeiro, P. López-Mahía, S. Muniategui-Lorenzo, E. Fernández-Fernández, D. Prada-Rodríguez, A. Moreda-Piñeiro, A. Bermejo-Barrera, P. Bermejo-Barrera, Pressurized liquid extraction of organometals and its feasibility for total metal extraction, TrAC, Trends Anal. Chem. 25 (2006) 511–519.
[32] K. Bluemlein, A. Raab, J. Feldmann, Stability of arsenic peptides in plant extracts: off-line versus on-line parallel elemental and molecular mass spectrometric detection for liquid chromatographic separation, Anal. Bioanal. Chem. 393 (2009) 357–366.
[33] Q. Zhao, Y. Liang, H. Yuan, Z. Sui, Q. Wu, Z. Liang, L. Zhang, Y. Zhang, Biphasic microreactor for efficient membrane protein pretreatment with a combination of formic acid assisted solubilization, on-column pH adjustment, reduction, alkylation, and tryptic digestion, Anal. Chem. 85 (2013) 8507–8512.
[34] Gajdosechova, M.M. Lawan, D.S. Urgast, A. Raab, K.G. Scheckel, E. Lombi, P. M. Kopittke, K. Loeschner, E.H. Larsen, G. Woods, In vivo formation of natural HgSe nanoparticles in the liver and brain of pilot whales, Sci. Rep. 6 (2016) 1–11.
[35] A. Manceau, A.-C. Gaillot, P. Glatzel, Y. Cherel, P. Bustamante, In vivo formation of HgSe nanoparticles and Hg–tetraselenolate complex from methylmercury in seabirds—implications for the Hg–Se antagonism, Environ. Sci. Technol. 55 (2021) 1515–1526.
[36] A. Manceau, J.-P. Bourdineaud, R.B. Oliveira, S.L. Sarrazin, D.P. Krabbenhoft, C. A. Eagles-Smith, J.T. Ackerman, A.R. Stewart, C. Ward-Deitrich, M.E. del Castillo Busto, Demethylation of methylmercury in bird, fish, and earthworm, Environ. Sci. Technol. 55 (2020) 1527–1534.
[37] M. Korbas, J.L. O'Donoghue, G.E. Watson, I.J. Pickering, S.P. Singh, G.J. Myers, T. W. Clarkson, G.N. George, The chemical nature of mercury in human brain following poisoning or environmental exposure, ACS Chem. Neurosci. 1 (2010) 810–818.
[38] A. Manceau, S. Azemard, L. Hédouin, E. Vassileva, D. Lecchini, C. Fauvelot, P. W. Swarzenski, P. Glatzel, P. Bustamante, M. Metian, Chemical forms of mercury in

blue marlin billfish: implications for human exposure, Environ. Sci. Technol. Lett. 8 (2021) 405–411.
[39] Y. Suzuki, M. Kondo, H. Akiyama, Y. Ogra, Presence of nano-sized mercury-containing particles in seafoods, and an estimate of dietary exposure, Environ. Pollut. 307 (2022), 119555.
[40] E. Nakazawa, T. Ikemoto, A. Hokura, Y. Terada, T. Kunito, S. Tanabe, I. Nakai, The presence of mercury selenide in various tissues of the striped dolphin: evidence from μ-XRF-XRD and XAFS analyses, Metallomics 3 (2011) 719–725.
[41] Y. Tanaka, H. Usuzawa, M. Yoshida, K. Kumagai, K. Kobayashi, S. Matsuyama, T. Inoue, A. Matsunaga, M. Shimura, J. Ruiz Encinar, Formation mechanism and toxicological significance of biogenic mercury selenide nanoparticles in human hepatoma HepG2 cells, Chem. Res. Toxicol. 34 (2021) 2471–2484.
[42] E. Bolea-Fernandez, A. Rua-Ibarz, E.M. Krupp, J. Feldmann, F. Vanhaecke, High-precision isotopic analysis sheds new light on mercury metabolism in long-finned pilot whales (Globicephala melas), Sci. Rep. 9 (2019) 7262.
[43] S. Queipo-Abad, Z. Pedrero, C. Marchán-Moreno, K. El Hanafi, S. Bérail, W. T. Corns, Y. Cherel, P. Bustamante, D. Amouroux, New insights into the biomineralization of mercury selenide nanoparticles through stable isotope analysis in giant petrel tissues, J. Hazard Mater. 425 (2022), 127922.
[44] B.A. Poulin, S.E. Janssen, T.J. Rosera, D.P. Krabbenhoft, C.A. Eagles-Smith, J. T. Ackerman, A.R. Stewart, E. Kim, Z. Baumann, J.-H. Kim, Isotope fractionation from in vivo methylmercury detoxification in waterbirds, ACS Earth Space Chem 5 (2021) 990–997.
[45] M. Renedo, Z. Pedrero, D. Amouroux, Y. Cherel, P. Bustamante, Mercury isotopes of key tissues document mercury metabolic processes in seabirds, Chemosphere 263 (2021), 127777.
[46] S. Clémens, M. Monperrus, O.F.X. Donard, D. Amouroux, T. Guérin, Mercury speciation analysis in seafood by species-specific isotope dilution: method validation and occurrence data, Anal. Bioanal. Chem. 401 (2011) 2699–2711.
[47] F. Laborda, A.C. Gimenez-Ingalaturre, E. Bolea, J.R. Castillo, About detectability and limits of detection in single particle inductively coupled plasma mass spectrometry, Spectrochim. Acta Part B At. Spectrosc. 169 (2020), 105883.
[48] H.E. Pace, N.J. Rogers, C. Jarolimek, V.A. Coleman, C.P. Higgins, J.F. Ranville, Determining transport efficiency for the purpose of counting and sizing nanoparticles via single particle inductively coupled plasma mass spectrometry, Anal. Chem. 83 (2011) 9361–9369.
[49] R. Peters, Z. Herrera-Rivera, A. Undas, M. van der Lee, H. Marvin, H. Bouwmeester, S. Weigel, Single particle ICP-MS combined with a data evaluation tool as a routine technique for the analysis of nanoparticles in complex matrices, J. Anal. At. Spectrom. 30 (2015) 1274–1285.
[50] A.F. de Oliveira, C.S. da Silva, S.R. Bianchi, A.R.A. Nogueira, The use of diluted formic acid in sample preparation for macro- and microelements determination in foodstuff samples using ICP OES, J. Food Compos. Anal. 66 (2018) 7–12.
[51] Y. Sun, Y. Yang, F.-Y. Tou, Z.-S. Niu, X.-P. Guo, C. Liu, J. Yan, J.-Y. Wu, M. Xu, L.-J. Hou, Extraction and quantification of metal-containing nanoparticles in marine shellfish based on single particle inductively coupled plasma-mass spectrometry technique, J. Hazard Mater. 424 (2022), 127383.
[52] M.V. Taboada-López, S. Iglesias-López, P. Herbello-Hermelo, P. Bermejo-Barrera, A. Moreda-Piñeiro, Ultrasound assisted enzymatic hydrolysis for isolating titanium dioxide nanoparticles from bivalve mollusk before sp-ICP-MS, Anal. Chim. Acta 1018 (2018) 16–25.
[53] I. López, S. Cuello, C. Camara, Y. Madrid, Approach for rapid extraction and speciation of mercury using a microtip ultrasonic probe followed by LC–ICP-MS, Talanta 82 (2010) 594–599.
[54] A.I. Cabañero, Y. Madrid, C. Camara, Enzymatic probe sonication extraction of Se in animal-based food samples: a new perspective on sample preparation for total and Se speciation analysis, Anal. Bioanal. Chem. 381 (2005) 373–379.
[55] Z. Xiao, S. Li, J. Guo, Z. Rao, C. Liu, Z. Jia, D. Suo, S. Wang, Y. Li, X. Fan, Application of enzymatic probe sonication for selenium speciation in animal feeds, J. Chromatogr. A 1530 (2017) 51–58.
[56] L.-L. Li, Y.-H. Cui, L.-Y. Lu, Y.-L. Liu, C.-J. Zhu, L.-J. Tian, W.-W. Li, X. Zhang, H. Cheng, J.-Y. Ma, Selenium stimulates cadmium detoxification in Caenorhabditis elegans through thiols-mediated nanoparticles formation and secretion, Environ. Sci. Technol. 53 (2019) 2344–2352.
[57] I. Gallien, F. Caurant, M. Bordes, P. Bustamante, P. Miramand, B. Fernandez, N. Quellard, P. Babin, Cadmium-containing granules in kidney tissue of the Atlantic white-sided dolphin (Lagenorhyncus acutus) off the Faroe Islands, Comp. Biochem. Physiol., Part C: Toxicol. Pharmacol. 130 (2001) 389–395.
[58] Z. Gajdosechova, A. Brownlow, N.T. Cottin, M. Fernandes, F.L. Read, D.S. Urgast, A. Raab, J. Feldmann, E.M. Krupp, Possible link between Hg and Cd accumulation in the brain of long-finned pilot whales (Globicephala melas), Sci. Total Environ. 545 (2016) 407–413.
[59] J. Gailer, Arsenic–selenium and mercury–selenium bonds in biology, Coord. Chem. Rev. 251 (2007) 234–254.